Characterization of a Perirectal Artifact in ^{18}F-FDG PET/CT

Martin A. Lodge[1], Muhammad A. Chaudhry[1], Don N. Udall[1], and Richard L. Wahl[1,2]

[1]*Division of Nuclear Medicine, Russell H. Morgan Department of Radiology and Radiological Sciences, Johns Hopkins University School of Medicine, Baltimore, Maryland; and* [2]*Sidney Kimmel Comprehensive Cancer Center at Johns Hopkins, Johns Hopkins University School of Medicine, Baltimore, Maryland*

Assessing tumor involvement in the rectal region can sometimes be complicated by what appears to be an artifact on ^{18}F-FDG PET/CT images. This artifact manifests as a high-intensity region on the PET image, extending posterior to the bladder in the area around the rectum. The aim of this study was to describe this artifact, which—as far as we are aware—has not been previously reported, and to investigate its cause. **Methods:** One hundred ^{18}F-FDG PET/CT studies (ordered-subsets expectation maximization reconstruction, CT attenuation correction) of patients with no known malignancy in the pelvis were retrospectively reviewed. Localized regions of apparently high uptake posterior to the bladder were considered an artifact when there was a discrepancy between attenuation-corrected (asymmetric appearance) and non–attenuation-corrected images (symmetric appearance). In addition, an experiment was performed using a body phantom containing 2 cylindric inserts simulating the bladder and a region of low-attenuation rectal gas. Attenuation-corrected images were reconstructed with different amounts of spatial misregistration intentionally introduced between the CT and PET images. **Results:** The artifact was observed in 15 of 100 patient studies and had a mean maximum standardized uptake value of 4.8 ± 2.7. When fused with sequentially acquired CT images, the artifact always appeared to be in the perirectal region near the bladder and an area of rectal gas. The phantom study indicated this artifact was consistent with an attenuation-correction problem caused by misregistration between CT and PET. Movement of gas within the rectum can cause an air pocket to be present during the PET acquisition at a location where CT indicated soft tissue. The resulting localized overcorrection for attenuation at the margin of the rectum and the extremely high activity concentration in the nearby bladder contributed to the artifact. **Conclusion:** Movement of gas within the rectum between acquisition of CT and PET images can lead to an artifact in attenuation-corrected PET images in the perirectal region. An awareness of this artifact and reference to non–attenuation-corrected images will aid in the interpretation of ^{18}F-FDG pelvis studies.

Key Words: PET/CT; artifact; attenuation correction; perirectal; bladder

J Nucl Med 2010; 51:1501–1506
DOI: 10.2967/jnumed.110.079145

Received May 13, 2010; revision accepted Jul. 20, 2010.
For correspondence or reprints contact: Martin A. Lodge, Division of Nuclear Medicine, Russell H. Morgan Department of Radiology and Radiological Sciences, Johns Hopkins University School of Medicine, 600 N. Wolfe St., Baltimore, MD 21287.
E-mail: mlodge1@jhmi.edu

PET is a useful tool for detecting, staging, and restaging carcinoma of the rectum. Accurate staging of patients with colorectal cancer is crucial for defining appropriate treatment and long-term prognosis. Accurate delineation of the primary tumor can be helpful in radiation treatment planning for such lesions. Local therapies can cure some limited rectal cancers, especially if the disease is early stage (*1–3*). Thirty percent to 40% of patients with rectal cancer present with nodal metastatic disease (*4*), which frequently involves lymph nodes along the lateral pelvic chain (obturator, internal iliac, and medial to external iliac artery) and inferior mesenteric artery in the mesorectal region. Immediate perirectal lymph nodes can also be involved with tumor. Low rectal cancers can also metastasize to the inguinal lymph nodes. Nodal tumor involvement is associated with poorer prognosis, higher incidence of local recurrence, and reduced survival (*5,6*). Currently, morphologic imaging with CT and MRI is mainly used for nodal disease assessment; however, even with enlarged lymph nodes, it is difficult to distinguish between metastatic and reactive nodes. Small nodes with limited or micrometastatic disease are easily missed. Additionally, there is a higher frequency of micrometastasis involving nodes of normal size in patients with rectal cancer (*7*). Similarly, ^{18}F-FDG PET/CT has limited sensitivity for the detection of nodal disease due to small size of nodes, variable ^{18}F-FDG uptake, and higher ^{18}F-FDG uptake in adjacent structures including the bladder and sometimes physiologic uptake in the bowel (*8*). The assessment of ^{18}F-FDG PET/CT images can also be problematic in patients presenting with suspected recurrent disease after surgical management. It has been observed that physiologic uptake in displaced organs after surgery is usually at the site of or adjacent to the site of recurrence and leads to a higher false-positive rate (*9,10*).

Given the difficulty associated with interpreting PET/CT images of the pelvis, any technical problems that further complicate the issue are of concern. Before the clinical introduction of iterative image-reconstruction algorithms, pelvis studies were complicated by streak artifacts associated with filtered backprojection. These artifacts appeared as noisy streaks emanating from the high-activity bladder and have been substantially reduced with iterative reconstruction as a result of better statistical weighting of the data (*11*). Elimination of filtered backprojection streak arti-

facts, combined with the introduction of high-resolution CT-based attenuation correction, may have revealed a different artifact that was not previously evident. This artifact manifests as a high-intensity region extending posterior to the bladder in the area around the rectum and, as far as we are aware, has not been previously reported. Awareness of this issue is important because in certain circumstances the artifact may complicate the assessments of lymph node involvement or postsurgical local recurrence.

This paper describes the appearance of this perirectal artifact and provides clinical examples. The incidence of the artifact has been estimated, and its magnitude has been quantified in terms of standardized uptake value. To clarify the mechanism underlying the artifact, we performed a phantom study that mimicked the environment encountered during ^{18}F-FDG studies of the pelvis. The aim of this work was to better understand the effect and increase awareness of what could be a potential source of erroneous overassessment of tumor in ^{18}F-FDG PET/CT studies of the pelvis.

MATERIALS AND METHODS

Patient Studies

To characterize the suspected artifact and estimate its incidence, patient data were retrospectively reviewed. One hundred thirty consecutively acquired clinical whole-body ^{18}F-FDG oncology studies were considered. To focus on image artifacts and minimize potential complications due to actual tumor, patients with known malignancy in the pelvis were excluded from further analysis. Data were acquired according to standard protocols using 2 different PET/CT systems (GE Healthcare). Seventy-one patients were studied using a Discovery LS (*12*), and 59 patients were studied using a Discovery VCT (RX) (*13*). After a 4-h fast and serum glucose measurement, patients were administered 8.1 MBq of ^{18}F-FDG per kilogram. Immediately before the start of scanning, patients were given the opportunity to void. The CT study occurred immediately before the PET study and involved data acquisition under shallow-breathing conditions. Whole-body PET data acquisition commenced at a level just below the pelvis. The median time between ^{18}F-FDG administration and the start of the PET acquisition was 61 min (SD, 13 min). Detailed acquisition parameters are summarized in Table 1.

The ordered-subsets expectation maximization algorithm was used to reconstruct all PET images. The 2-dimensional implementation on the Discovery LS used 2 iterations, 28 subsets, a 5.5-mm postreconstruction gaussian filter, and 3.9-mm pixels. The fully 3-dimensional implementation on the Discovery VCT (RX) used 2 iterations, 21 subsets, a 3.0-mm postreconstruction gaussian filter, and 4.7-mm pixels. All PET data were reconstructed with and without CT-based attenuation correction. Areas of high ^{18}F-FDG accumulation in the region posterior to the bladder were considered artifacts if their appearance on attenuation-corrected images was inconsistent with their appearance on non–attenuation-corrected (NAC) images. Specifically, an artifact was indicated if the transverse NAC image showed a symmetric pattern about the anterior–posterior axis passing through the mid rectum whereas the attenuation-corrected images showed a markedly asymmetric pattern. When an artifact was indicated, a manually positioned circular region of interest was used to identify the pixel with the maximum standardized uptake value (g/mL), which was used to quantify the magnitude of the effect. All images were analyzed on an Advantage Workstation (version 4.4; GE Healthcare). A single reader examined all studies for the presence of the artifact.

Phantom Studies

To investigate the effect of misregistration between the PET and CT images, a phantom experiment was performed in which different degrees of spatial misalignment were intentionally introduced. The phantom attempted to mimic the situation frequently encountered in the pelvis, where high activity concentrations in the bladder are located close to regions of rectal gas. By shifting the PET and CT images with respect to each other, the experiment simulated the situation in which rectal gas was displaced between the 2 acquisitions, leading to incorrect attenuation correction of the PET data.

The experimental study used the body phantom of the National Electrical Manufacturers Association and International Electrotechnical Commission (*14*), with the spheric inserts removed. A 5-cm-diameter cylinder containing no activity and a low-attenuation medium (−640 Hounsfield units) was positioned centrally within the phantom, simulating a region of rectal gas (identical to the

TABLE 1. PET/CT Acquisition Parameters for Discovery LS and Discovery VCT (RX) PET/CT Systems

Acquisition parameter	Discovery LS	Discovery VCT (RX)
CT slice configuration	4-slice	64-slice
CT pitch	1.5	0.984
CT tube voltage	120 kVp	120 kVp
CT tube current	20–200 mA*	20–200 mA*
CT rotation time	0.8 s	0.5 s
PET detector material	Bismuth germanate	Lutetium yttrium orthosilicate
PET acquisition mode	2 dimensions	3 dimensions
PET scan time per bed position	300 s	255 s
PET bed position overlap	3 slices (13 mm)	11 slices (36 mm)
PET coincidence window	12.5 ns	6.5 ns
PET randoms correction	Delayed channel	Singles
PET energy range	300–650 keV	425–650 keV

*Tube current automatically determined as a function of patient size. One hundred thirty milliamperes used for phantom study.

lung insert of the NEMA NU 2-2007 image quality protocol). A second cylinder, also 5 cm in diameter, was placed immediately adjacent and anterior to the first cylinder. This second cylinder was filled with ^{18}F-FDG in an aqueous mixture and simulated the bladder. The phantom background region was also filled with an aqueous mixture of ^{18}F-FDG and thus had the same attenuation properties as the bladder insert. At the time of scanning, the bladder cylinder had an activity concentration of 216 kBq/mL, and the background region had an activity concentration of 2.4 kBq/mL. Both activity concentrations were typical of values observed in clinical oncology ^{18}F-FDG studies at our center.

Image data were acquired on the Discovery VCT (RX) PET/CT system using a protocol typically used for whole-body oncology studies. CT was acquired for attenuation correction, followed without any intervention by PET. PET images were reconstructed using the previously described clinical protocol, with and without attenuation correction. Multiple attenuation-corrected images were reconstructed with lateral displacements of 0, 5, 10, 15, and 20 mm applied in software to the PET data relative to the CT data (Fig. 1). Artifacts were quantified by dividing both the maximum pixel value and the minimum pixel value by the mean activity concentration in the background. This background activity concentration was measured using five 40-mm-diameter circular regions of interest placed in the image that was attenuation-corrected using perfectly aligned CT.

RESULTS

Patient Studies

Of the 130 patients initially considered, 30 were excluded from further analysis because they had known disease in the pelvis including ovarian cancer, colorectal cancer, rectal cancer, vagina adenocarcinoma, bladder rhabdomyosarcoma, uterine cancer, and prostate cancer. The remaining 100 patients included those with lymphoma (n = 24), lung cancer (n = 13), breast cancer (n = 12), oral cancer (n = 8), squamous cell cancer (n = 7), pancreatic cancer (n = 5), esophageal cancer (n = 4), head and neck cancer (n = 2), and other indications (n = 25).

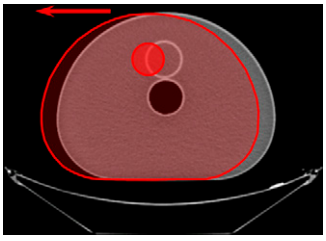

FIGURE 1. CT image showing 2 cylindric inserts within larger body phantom. Upper cylinder and outer background region contained radioactive water, whereas lower cylinder contained no activity and consisted of low-attenuation medium designed to simulate a pocket of rectal gas. Superimposed in red on CT is a diagram illustrating how the emission distribution was displaced relative to CT before attenuation correction. Lateral displacements of 5, 10, 15, and 20 mm were considered. These displacements were implemented in software, and the phantom was not physically moved between CT and PET acquisitions (apart from bed translation that moved phantom from CT to PET gantries).

Of these 100 patient studies, 15 exhibited tracer accumulation in the perirectal region that was considered to be artifacts. Examples of these artifacts are shown in Figure 2. The artifact appeared as a region of apparently high tracer accumulation extending posterior to the bladder in the attenuation-corrected images, with no corresponding focus in the NAC images. In all 15 studies, the artifact was located in the perirectal region, immediately adjacent to a region of rectal gas, and was not observed when rectal gas was absent. The mean maximum standardized uptake value within the artifact was 4.8 (range, 2.0–13.2; SD, 2.7). Of the 15 studies in which artifacts were observed, 8 were acquired on the Discovery LS and the remaining 7 were acquired on the Discovery VCT (RX).

Phantom Studies

Figure 3 shows how the phantom experiment was able to reproduce the artifact observed in clinical images. Figures 3A and 3B show attenuation-corrected PET and PET/CT images from a clinical study that displayed the artifact. The attenuation-corrected image (Fig. 3A), compared with the NAC image, exhibited asymmetry (Fig. 3C). Figure 3D shows a phantom image, attenuation-corrected using CT data that were misregistered by 10 mm with respect to the PET data. The artifact in Figures 3D and 3E closely resembles the artifact seen in Figures 3A and 3B. Figure 3F shows an image derived from the same PET phantom data but this time attenuation-corrected using correctly aligned CT. No evidence of the artifact is visible in Figures 3F or 3G, confirming that misregistration was the source of the artifact. In addition to the expected attenuation artifacts, the image in Figure 3H shows symmetry posterior to the bladder insert that is similar to the corresponding clinical image (Fig. 3C).

Figure 4 shows phantom data that illustrate how the high-activity artifact increased with increasing misregistration of the PET and CT images. For the 90-to-1 bladder-to-background activity concentration ratio simulated here, the artifact had a maximum-activity concentration that was greater than the background by factors of 3.4 ± 0.002, 5.3 ± 0.1, 7.1 ± 0.1, and 8.9 ± 0.1 for lateral misalignments of 5, 10, 15, and 20 mm, respectively. Also, on the opposite side of the air-filled insert there was a corresponding low-intensity artifact that became more apparent as the spatial misregistration increased. The minimum-activity concentration in this region was less than the background by factors of 0.26 ± 0.04, 0.12 ± 0.01, 0.06 ± 0.004, and 0.039 ± 0.002 for lateral misalignments of 5, 10, 15, and 20 mm, respectively.

DISCUSSION

In this paper, we describe an image artifact that has been observed in ^{18}F-FDG PET/CT studies and can potentially complicate interpretation by suggesting tumor involvement is present in the rectum or perirectal areas when it is not. Phantom studies indicated that the artifact was caused by

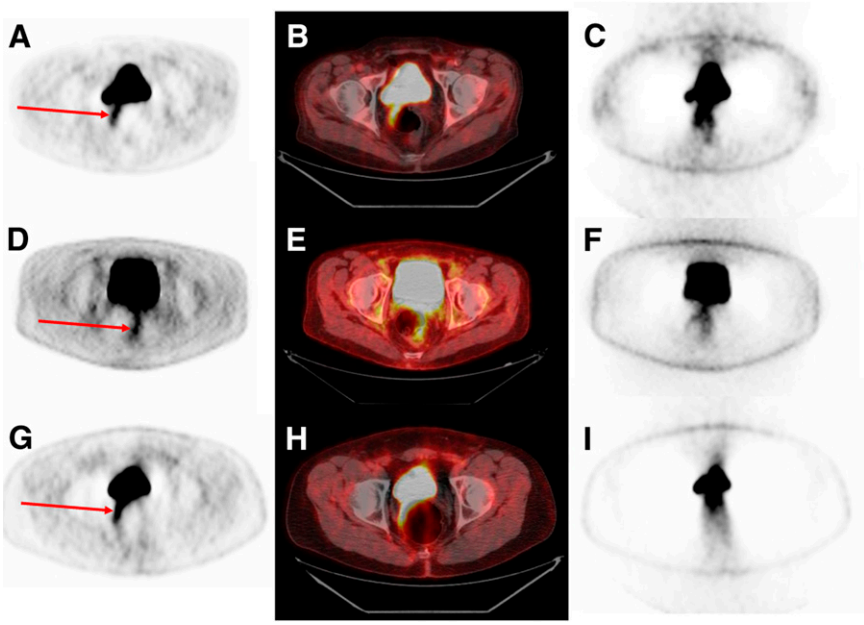

FIGURE 2. Example images from ^{18}F-FDG PET/CT studies performed on 3 separate patients. Artifact is indicated by arrows. Attenuation-corrected PET is shown in A, D, and G. Attenuation-corrected PET, fused with corresponding CT, is shown in B, E, and H. NAC PET is shown in C, F, and I.

attenuation-correction error due to motion between the CT and PET acquisitions. Although gross patient motion may potentially contribute, visual assessment of the fused PET/CT images did not indicate that the patients shifted their position on the bed during the imaging procedure. Instead, the images suggest that movement of gas within the rectum led to differences in the attenuation distribution between CT and PET acquisitions. This is supported by the fact that in the group of patients studied, the artifact was never seen in cases in which pockets of rectal gas were absent.

We hypothesized that the gas pocket shifted between the CT and PET acquisitions such that low-attenuation gas was present during the PET acquisition at a location where the previously acquired CT scan indicated relatively high-attenuation soft tissue. For example, in Figure 3B the pocket of rectal gas may have shifted from the patient's left to right (right to left when viewing the figure) between the CT and PET acquisitions. As a result, the PET data were overcorrected for attenuation at the location where CT indicated soft tissue but was actually low-attenuation gas at the time that the PET image was acquired. Compounding this issue was the fact that in these ^{18}F-FDG studies, the bladder typically contained large amounts of tracer in high activity concentrations. Overcorrection for attenuation for projec-

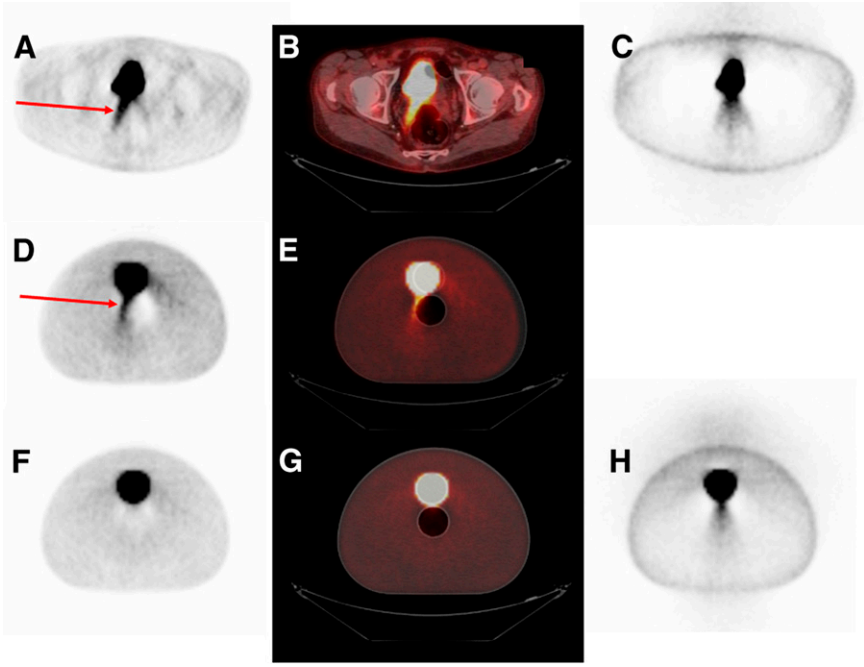

FIGURE 3. Example clinical and phantom images showing artifact indicated by arrows in A and D. (A) Attenuation-corrected clinical PET study. (B) Image in A superimposed on CT in fused display. (C) NAC clinical PET. (D) Phantom image attenuation-corrected using CT data that were misregistered by 10 mm. (E) Image in D superimposed on CT in fused display. (F) Phantom image attenuation-corrected using correctly aligned CT data. (G) Image in F superimposed on CT in fused display. (H) NAC phantom PET.

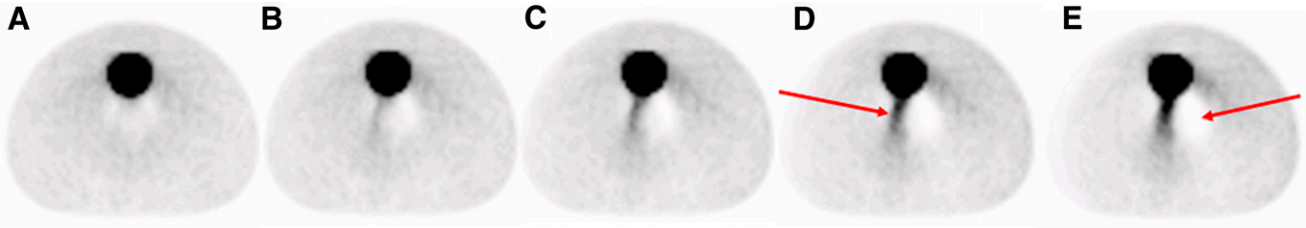

FIGURE 4. Phantom images attenuation-corrected with different amounts of lateral misregistration introduced between PET and CT data. Image in A was attenuation-corrected using perfectly registered PET and CT, but images in B, C, D, and E had misregistrations of 5, 10, 15, and 20 mm, respectively. Arrows in D and E indicate hot and cold artifacts, respectively, although similar artifacts are present in B–E.

tions passing through the bladder resulted in the characteristic artifacts described in this paper.

The phantom experiment provided strong evidence supporting attenuation mismatch as the cause of this artifact. Figure 4A shows that there was no indication of the artifact when the PET data were attenuation-corrected using perfectly aligned CT. However, as the PET data were shifted relative to the low-attenuation cylinder simulating rectal gas, the artifact was introduced (Figs. 4B–4E). Striking similarity between the artifact in the phantom and clinical cases was observed. Also, particularly in Figure 4E, there were distortions toward the edges of the phantom that arose because of the misregistration of the CT and PET data. In the clinical situation of interest here, spatial misregistration is due to motion of the internal organs as opposed to gross patient motion. As such, these edge effects in the phantom images are not representative of patient imaging. A slightly more realistic phantom arrangement might involve adjusting the relative position of the internal organ compartments between CT and PET data acquisition. Although this change in relative position has the potential to reduce these edge effects, adjusting the phantom configuration in this way may make it more difficult to accurately control the extent of the misregistration. For this reason, software manipulation was preferred in the present study.

Other different, but related, artifacts due to motion between CT and PET acquisitions have been reported in the literature (*15–17*). Artifacts frequently occur around the lung–soft-tissue interface, where there is a pronounced discontinuity in the local attenuation properties, coupled with a high likelihood for spatial misalignment due to respiratory motion. In both oncology and cardiology applications, the tissue of primary interest is usually either solid tumor or myocardium, as opposed to lung. When motion problems occur, the most noticeable effect arises when regions of soft tissue are incorrectly attenuation-corrected as if they were located in lung. The resulting undercorrection for attenuation can potentially reduce tumor uptake measurements (*18*) or introduce apparent defects in myocardial images (*19*). In the present study, we see an example of the opposite effect: overcorrection of a region of low-attenuation gas with factors appropriate for higher-attenuation soft tissue. When this overcorrection occurs in regions surrounded by low tracer accumulation, it results in only minor increases in apparent tracer activity concentration (*20*). However, as we have demonstrated, overestimated attenuation correction can lead to a characteristic high-activity artifact in the region around the bladder due to the extremely high activity concentrations encountered there. Although not obvious in the clinical images, the phantom images also showed a related low-activity artifact that corresponded to the other side of the air pocket where attenuation correction was underestimated.

Although further work with other scanner systems is warranted, the artifact does not seem to be related to the PET acquisition mode. In this study, we observed the artifact in images acquired on 2 generations of PET system: those using bismuth germanate detectors and 2-dimensional acquisition and those using lutetium yttrium orthosilicate detectors and 3-dimensional acquisition. There is some scope for reducing the occurrence of the artifact. Diuretics or bladder catheterization can be used to decrease radioactivity in the bladder and will likely reduce the magnitude of the artifact. Software corrections involving retrospective nonlinear registration of the PET and CT images may also provide a potential, albeit quite cumbersome, mechanism for eliminating these artifacts. However, possibly the best approach to managing this artifact is to be aware of its appearance and refer to NAC images when the artifact is suspected.

This artifact is of greatest relevance in patients who have had carcinoma of the rectum in whom an apparent ^{18}F-FDG signal due to artifacts must not be confused with residual tumor. Similarly, familiarity with this artifact will reduce the possibility of a false-positive diagnosis of rectal or perirectal tumor.

CONCLUSION

In attenuation-corrected PET images, movement of gas within the rectum can lead to an artifact of apparently increased radiotracer uptake in the perirectal region that can potentially complicate interpretation by suggesting the presence of rectal wall or perirectal tumor. An awareness

of this artifact and reference to NAC images will aid interpretation of PET/CT pelvis studies.

REFERENCES

1. Gearhart SL, Frassica D, Rosen R, Choti M, Schulick R, Wahl R. Improved staging with pretreatment positron emission tomography/computed tomography in low rectal cancer. *Ann Surg Oncol.* 2006;13:397–404.
2. Capirci C, Rubello D, Chierichetti F, et al. Long-term prognostic value of ^{18}F-FDG PET in patients with locally advanced rectal cancer previously treated with neoadjuvant radiochemotherapy. *Am J Roentgenol.* 2006;187:W202–W208.
3. Bassi MC, Turri L, Sacchetti G, et al. FDG-PET/CT imaging for staging and target volume delineation in preoperative conformal radiotherapy of rectal cancer. *Int J Radiat Oncol Biol Phys.* 2008;70:1423–1426.
4. Takahashi T, Ueno M, Azekura K, Ohta H. Lateral node dissection and total mesorectal excision for rectal cancer. *Dis Colon Rectum.* 2000;43(suppl 10):S59–S68.
5. Hida J, Yasutomi M, Fujimoto K, Maruyama T, Okuno K, Shindo K. Does lateral lymph node dissection improve survival in rectal carcinoma? Examination of node metastases by the clearing method. *J Am Coll Surg.* 1997;184:475–480.
6. Steup WH, Moriya Y, van de Velde CJ. Patterns of lymphatic spread in rectal cancer: a topographical analysis on lymph node metastases. *Eur J Cancer.* 2002;38:911–918.
7. Bjelovic M, Kalezic V, Petrovic M, et al. Correlation of macroscopic and histological characteristics in the regional lymph nodes of patients with rectal and sigmoidal adenocarcinoma. *Hepatogastroenterology.* 1998;45:433–438.
8. Llamas-Elvira JM, Rodriguez-Fernandez A, Guitierrez-Sainz J, et al. Fluorine-18 fluorodeoxyglucose PET in the preoperative staging of colorectal cancer. *Eur J Nucl Med Mol Imaging.* 2007;34:859–867.
9. Even-Sapir E, Parag Y, Lerman H, et al. Detection of recurrence in patients with rectal cancer: PET/CT after abdominoperineal or anterior resection. *Radiology.* 2004;232:815–822.
10. Keogan MT, Lowe VJ, Baker ME, McDermott VG, Lyerly HK, Coleman RE. Local recurrence of rectal cancer: evaluation with F-18 fluorodeoxyglucose PET imaging. *Abdom Imaging.* 1997;22:332–337.
11. Lonneux M, Borbath I, Bol A, et al. Attenuation correction in whole-body FDG oncological studies: the role of statistical reconstruction. *Eur J Nucl Med.* 1999;26:591–598.
12. DeGrado TR, Turkington TG, Williams JJ, et al. Performance characterization of a whole-body PET scanner. *J Nucl Med.* 1994;35:1398–1406.
13. Kemp BJ, Kim C, Williams JJ, et al. NEMA NU 2-2001 performance measurements of an LYSO-based PET/CT system in 2D and 3D acquisition modes. *J Nucl Med.* 2006;47:1960–1967.
14. National Electrical Manufacturers Association (NEMA). *Performance Measurements of Positron Emission Tomographs*. NEMA standards publication NU2-2007. Rosslyn, VA: NEMA; 2007.
15. Osman MM, Cohade C, Nakamoto Y, Marshall LT, Leal JP, Wahl RL. Clinically significant inaccurate localization of lesions with PET/CT: frequency in 300 patients. *J Nucl Med.* 2003;44:240–243.
16. Goerres GW, Burger C, Kamel E, et al. Respiration-induced attenuation artifact at PET/CT: technical considerations. *Radiology.* 2003;226:906–910.
17. Martinez-Moller A, Souvatzoglou M, Navab N, Schwaiger M, Nekolla SG. Artifacts from misaligned CT in cardiac perfusion PET/CT studies: frequency, effects, and potential solutions. *J Nucl Med.* 2007;48:188–193.
18. Pan T, Mawlawi O, Nehmeh SA, et al. Attenuation correction of PET images with respiration-averaged CT images in PET/CT. *J Nucl Med.* 2005;46:1481–1487.
19. Gould KL, Pan T, Loghin C, Johnson NP, Guha A, Sdringola S. Frequent diagnostic errors in cardiac PET/CT due to misregistration of CT attenuation and emission PET images: a definitive analysis of causes, consequences, and corrections. *J Nucl Med.* 2007;48:1112–1121.
20. Nakamoto Y, Chin BB, Cohade C, Osman M, Tatsumi M, Wahl RL. PET/CT: artifacts caused by bowel motion. *Nucl Med Commun.* 2004;25:221–225.